

# PROLONGED MINIMA AND THE 179-YR CYCLE OF THE SOLAR INERTIAL MOTION

RHODES W. FAIRBRIDGE

*Department of Geological Sciences, Columbia University, New York, NY 10027, U.S.A.*

and

JAMES H. SHIRLEY

*P.O. Box 169, Canoga Park, CA 91305, U.S.A.*

(Received 3 January, 1987)

**Abstract.** We employ the JPL long ephemeris DE-102 to study the inertial motion of the Sun for the period A.D. 760–2100. Defining solar orbits with reference to the Sun's successive close approaches to the solar system barycenter, occurring at mean intervals of 19.86 yr, we find simple relationships linking the inertial orientation of the solar orbit and the amplitude of the precessional rotation of the orbit with the occurrence of the principal prolonged solar activity minima of the current millenium (the Wolf, Spörer, and Maunder minima). The progression of the inertial orientation parameter is controlled by the 900-yr 'great inequality' of the motion of Jupiter and Saturn, while the precessional rotation parameter is linked with the 179-yr cycle of the solar inertial motion previously identified by Jose (1965). A new prolonged minimum of solar activity may be imminent.

## 1. Introduction

Solar activity varies with time, but the physical origins of this variability are as yet unknown. Periodicities of about 11, 22, 60, 80–90, and 180 yr are often reported (Cole, 1973; Currie, 1973; Cohen and Lintz, 1974; Kuklin, 1976; Lomb and Anderson, 1980; Sonett, 1982; Otaola and Zenteno, 1983; Fairbridge and Hameed, 1983; Gregg, 1984), but there appears to be nothing in the physical makeup of the Sun to explain why these particular periodicities should arise.

The occurrence of a number of prolonged minima of solar activity of the Maunder minimum type is by now well established (Eddy, 1976, 1983; Stuiver and Quay, 1980a), but the origins of this form of temporal variability are likewise unknown. In these episodes sunspot activity is suppressed, though apparently not entirely eliminated, for periods of 6–12 decades.

One approach to the problem of temporal variability of solar activity has returned encouraging results. This approach relates changes in solar activity with variations in the inertial motion of the Sun. The relationships uncovered to date have received little attention, however, as theory provides no straightforward explanation for the relationships found, and some studies have appeared in small journals and symposia. Thus there is need for a brief review of both (1) basic features of the solar motion, and (2) previous results. This is provided in Sections 3 and 4 of this paper.

In the present investigation we are concerned with the relationship, if any, of the solar motion and long-period fluctuations of solar activity as represented by the principal

prolonged minima of solar activity of the present millenium. Thus our first concern is to define the timing of episodes of interest.

## 2. Record of Solar Variation

In the course of this investigation we will compare periods of high solar activity with periods of strongly suppressed activity. To this end we have tabulated 11-yr solar cycle maxima with  $R_M > 100$  from the telescopic record, to represent higher activity periods. The dates of these maxima are given in Table I. While some authors estimate years of 11-yr cycle maxima for the pre-telescopic period (Wittmann, 1978; Schove, 1983), we have not included these in our tabulation due to uncertainties in amplitude and timing.

TABLE I  
Sunspot maxima,  $R_M > 100$ ,  
1700–present

1727.5	1870.6
1738.7	1917.6
1769.7	1937.4
1778.4	1947.5
1788.1	1957.9
1837.2	1968.9
1848.1	1979.9

The telescopic record includes the Maunder minimum (Maunder, 1894; Eddy, 1976, 1983). Also notable is the period 1798–1823, characterized by the lowest levels of activity of the period subsequent to the Maunder minimum. We propose to call this the ‘Sabine excursion’, after Sir Edward Sabine, who drew attention to this period of attenuated solar activity in the course of his investigations in the 1850’s.

Information on pre-telescopic solar variability comes from several sources. Many dated naked-eye observations are found in historical sources, particularly from the Orient (Clark and Stephenson, 1978; Clark, 1979). Historical sources are also employed to compile lists of auroral observations (Siscoe, 1980), which provide a valuable (but imperfect) index of past solar activity.

The longest continuous record of pre-telescopic solar variability is derived from measurements of the concentration of the isotope  $^{14}\text{C}$  in tree rings. Trees incorporate atmospheric carbon during growth, recording the concentrations of carbon isotopes present in the atmosphere at the time. Atmospheric  $^{14}\text{C}$  is formed in reactions initiated by cosmic ray bombardment in the upper atmosphere; the rate of  $^{14}\text{C}$  formation fluctuates inversely with the level of solar activity, and with the moment of the geomagnetic field. Thus higher  $^{14}\text{C}$  production rates correspond to periods of reduced solar activity.

Several investigators have published curves representing the time-variability of the

concentration of atmospheric  $^{14}\text{C}$  for the period 6000 B.C. – present, based on multiple measurements performed at different labs, and repeated employment of different source materials (Suess, 1980; Klein *et al.*, 1980, 1982; Neftel *et al.*, 1981; Damon and Linick, 1986). These show substantial agreement. Still for remote times a number of factors introduce uncertainties (Barton *et al.*, 1979; Stuiver and Quay, 1980a, b; Siegenthaler *et al.*, 1980; Lazear *et al.*, 1980; Klein *et al.*, 1982; Stuiver, 1982, 1983; Damon and Linick, 1986; Stuiver and Pearson, 1986). While the precision of measurements and chronologies is improving, consensus on the magnitude and timing of earlier Maunder minimum type excursions is yet to be attained.

A periodicity of between 150 and about 200 yr is an important feature of the radiocarbon record (Damon, 1977; de Jong *et al.*, 1979; Stuiver, 1980; Suess, 1980; de Jong and Mook, 1980; Neftel *et al.*, 1981; Pearson *et al.*, 1983; Sonett and Suess, 1984; Sonett, 1984; Suess, 1986; Damon and Linick, 1986). These variations were first noted by de Vries (1958); their association with solar activity was demonstrated by Stuiver (1961). The amplitude and period of these ‘Suess wiggles’ varies depending on the record, the analysis procedure, and interval of time evaluated (Sonett, 1984).

In the present investigation we consider only the most recent part of the radiocarbon record, which currently represents the most reliable portion for purposes of identifying past fluctuations of solar activity. We plan to extend the analysis to the earlier portions of the record at a later date.

TABLE II  
Prolonged sunspot minima

Maunder minimum	1645–1712
Spörer minimum	1411–1524
Wolf minimum	1281–1347

*Legend:* Starting and ending dates are years of 11-yr sunspot cycle minima, bracketing the prolonged minimum, from the observational record for the Maunder minimum and after Schöve (1983) for the Spörer and Wolf minima.

Table II lists the adopted dates of inception and termination of the principal prolonged minima of solar activity of the current millenium. These episodes have been recognized in the radiocarbon record, in auroral observations, and in the catalog of early telescopic and pre-telescopic sunspot observations. The starting and ending dates are years of 11-yr sunspot cycle minima bracketing the episode, from the observational record for the Maunder minimum and as estimated by Schöve (1983) for the Spörer and Wolf minima. Some authors note in addition an earlier episode near A.D. 1020, termed the ‘Oort minimum’ (Stuiver and Grootes, 1980; Eddy, 1983). This episode was, however, significantly shorter (20–40 yr?) and weaker (Stuiver, 1986) than the Wolf, Spörer, and Maunder minima.

### 3. Inertial Motion of the Sun

The center of gravity of a thrown dumbbell describes a regular arc, while the weighted ends undergo complex gyrations. Similarly the barycenter of our solar system follows a relatively regular path as we orbit the galactic center, while individual solar system bodies, particularly the Sun, describe complex orbits about the barycenter. The barycenter is the origin of the solar system inertial frame (the fundamental coordinate system of Newtonian dynamics).

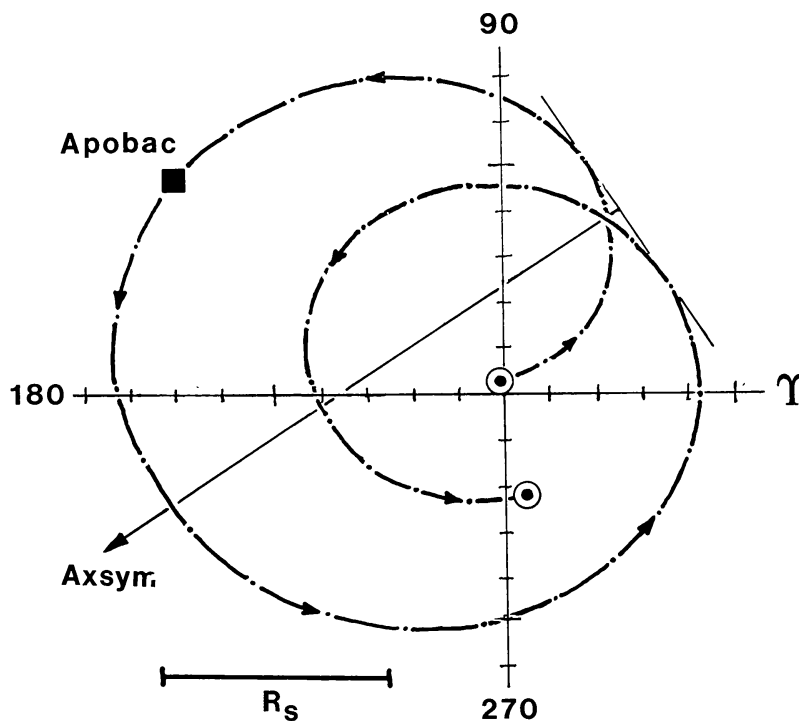


Fig. 1. Solar barycentric orbit A.D. 1990–2013. The solar system barycenter is the origin. The equator and equinox of 1950.0 provide the reference coordinate system in the JPL ephemeris DE-102. Here the reference plane parallels the equatorial plane of the Earth, with the vernal equinox  $\Upsilon$  at right ascension  $\alpha = 0^\circ$  (0 hours). Distances marked on the axes are in units of  $10^{-3}$  AU ( $1.496 \times 10^5$  km). The solar radius  $R_s$  ( $= 6.959 \times 10^5$  km) is shown for comparison. Points on the curve give the position of the center of the Sun, relative to the barycenter, at 200 day intervals. The starting and ending points of the curve are the peribacs of April 1990 and November 2013 (Julian dates 2448 000–2456 600). The apobac (time of maximum orbit radius) is denoted on the curve by  $\blacksquare$ . The axsym (defined in Section 5) is a measure of the orientation of the orbit in inertial space.

Figure 1 shows the path of the center of the Sun relative to the solar system barycenter for the period from 18 April, 1990 to 3 November, 2013. The points on the curve give the Sun position at time intervals of 200 days. The units marked on the axes are in  $\text{AU} \times 10^{-3}$  ( $1.496 \times 10^5$  km). The coordinates are from the JPL long ephemeris DE-102 (Newhall *et al.*, 1983).

An inertial coordinate frame for the solar system is one which originates in and moves with the barycenter, but which is otherwise ‘fixed in space’. The  $x - y$  plane of the

DE-102 is the Earth equatorial plane of 1950.0, with  $Y$  = vernal equinox (conventional origin of celestial longitudes and right ascension values). The 1950 equatorial plane is inclined by more than  $23^\circ$  to the ecliptic, which in turn has a small inclination to the invariable plane. In a previous investigation (Fairbridge and Sanders, 1987) the unmodified JPL equatorial Sun coordinates were employed in producing plots such as that of Figure 1. To check whether any significant distortion of the path was introduced by this choice, one of us (JS) has written a microcomputer program to replicate the JPL output, using formulae from Clemence (1953) and Van Flandern and Pulkkinen (1979). This program reproduces the JPL output over the time period of this study with errors typically in the range  $0-3 \times 10^{-5}$  AU, and also resolves the solar motion relative to ecliptic and invariable planes. Comparisons show that the distortion introduced by using the equatorial reference plane is negligible for purposes of this investigation.

The solar motion is driven by the changing configuration of the planets. The giant planets Jupiter, Saturn, Uranus, and Neptune are primarily responsible, and of these Jupiter and Saturn play a dominant role. More than 86% of total solar system angular momentum is concentrated in this pair. The 19.86-yr synodic period of Jupiter and Saturn (from one heliocentric conjunction to the next) is in consequence reflected most prominently in the inertial motion of the Sun; the Sun's motion is 'locked on' to this 'Saturn-Jupiter lap cycle' (SJL). Recognizing this relationship, Fairbridge and Sanders (1987) defined individual solar orbital cycles with reference to successive close approaches to the barycenter, which recur at mean intervals of 19.86 yr. In Figure 1 these close approach times, termed 'peribacs', are the starting and ending points of the path plotted. Other definitions of a solar orbital cycle are possible; Landscheidt (1983) for instance employs the time of greatest separation of the Sun and barycenter.

The solar motion differs from the Keplerian motion of planets and satellites in important ways. For instance, the velocity is largest when the distance separating the Sun and the barycenter is greatest (Figure 1). And, the solar orbital angular momentum  $L$ , with a magnitude  $\approx 10^{40}$  kg m<sup>2</sup> s<sup>-1</sup>, may vary by an order of magnitude over a period of  $\approx 10$  years (Blizard, 1981).

Table III lists definitions of several dynamical quantities which will be referenced in the discussion to follow.

#### 4. Previous Investigations

The question of a planetary influence on solar activity has a long history, beginning with investigations by Wolf and Carrington in the mid-19th century (Ferris, 1969). A number of workers present evidence of a relationship of solar activity and the positioning of planets (de La Rue *et al.*, 1872; Schuster, 1911; Nelson, 1951, 1954; Bigg, 1967). Others note a close correspondence of sunspot periodicities and planetary orbital period resonances (Bureau and Craine, 1970; Bagby, 1975; Wood, 1975; Mörth and Schlamming, 1979; Blizard, 1981).

The hypothesis of a planetary *tidal* influence on solar activity is understandably regarded with skepticism, as the tidal forces at the surface of the Sun are about  $10^{12}$

TABLE III  
Dynamical functions

$R = (x^2 + y^2 + z^2)^{1/2}$	Distance from Sun's center to solar system barycenter (Jose, 1965)
$V = (\dot{x}^2 + \dot{y}^2 + \dot{z}^2)^{1/2}$	Velocity (Jose, 1965)
$\rho = V^3 / [(\dot{y}\ddot{z} - \dot{z}\ddot{y})^2 + (\dot{z}\ddot{x} - \dot{x}\ddot{z})^2 + (\dot{x}\ddot{y} - \dot{y}\ddot{x})^2]^{1/2}$	Radius of curvature of Sun's path (Jose, 1965)
$P = \rho V$	Angular momentum about the instantaneous center of curvature (Jose, 1965)
$dP/dt$	Rate of change of $P$ (Jose, 1965)
$L = [(y\dot{z} - z\dot{y})^2 + (z\dot{x} - x\dot{z})^2 + (x\dot{y} - y\dot{x})^2]^{1/2}$	Angular momentum about solar system barycenter (Jose, 1965)
$T = \tau = dL/dt$	Rate of change of angular momentum about barycenter ('torque') (Jose, 1965)
$dT/dt = d^2L/dt^2$	Rate of change of $T$ (Landscheidt, 1983)
$\Delta L = \int_{t_0}^{t_1} T(t) dt$	Time-integral of torque (measures impulses of $L$ ) (Landscheidt, 1981)

Note: Other functions are listed in Pimm and Bjorn (1969), Wood and Wood (1965), and Jose (1965).

times smaller than the solar gravity there. While some investigators have reported correlations of planetary tides and solar activity (Suda, 1962; Takahashi, 1968; Wood, 1972), others have reported null results (Dingle *et al.*, 1973; Okal and Anderson, 1975; Smythe and Eddy, 1977). The analysis by Okal and Anderson (1975) is particularly convincing; these authors computed the full tidal problem for the Sun, finding no relationship of solar activity and tidal potential.

It is very important to distinguish between planetary tidal studies and studies relating to the solar orbital motion. The solar motion plotted in Figure 1 is a phenomenon bearing little or no relationship to solar tidal variations. The accelerations of the solar motion (Wood and Wood, 1965) are orders of magnitude larger than the tidal accelerations.

Arriaga (1955), Wood and Wood (1965), Jose (1965), Pimm and Bjorn (1969), and Landscheidt (1981, 1983) present evidence of a relationship linking the solar motion and solar activity. Of these the studies by Jose (1965) and Landscheidt (1981, 1983) are of particular interest.

Jose (1965) studied the solar motion for the years 1653–2060, comparing this with the record of solar activity to 1964. He found a remarkable correspondence of curves of the rate of change of solar orbital angular momentum ( $dL/dt$ ) and the rate of change

of angular momentum about the instantaneous center of curvature ( $dP/dt$ ) and sunspot numbers. In addition he noted a fundamental repetition period of 178.7 yr in the curves for  $R$ ,  $\rho$ ,  $dL/dt$ , and  $dP/dt$  (Table III); his curves for 1655–1833 are remarkably similar to those for 1833–2012.

Landscheidt (1981) noted that the largest fluctuations of  $dL/dt$  take place when the Sun's center passes near the barycenter. He calculated the strength of these impulses ( $\Delta L$ , Table III) and found a relationship linking successive strong impulses with the phase of the 80–90 yr secular Gleissberg cycle of solar activity since 1700 (Landscheidt, 1981, Figure 2). He noted in addition a correspondence in time of the strongest impulses and prolonged solar activity minima identified in the 8000-yr  $^{14}\text{C}$  curve published by Eddy (1977).

Landscheidt (1983) later employed the less cumbersome  $dT/dt$  to identify the times and amplitudes of impulsive changes in the solar motion. Cross correlation of yearly values of  $dT/dt$  and sunspot numbers yielded significant positive correlation at 11, 22, and 31 yr. Sunspot numbers lag the  $dT/dt$  curve by about 5.5 yr. And, the extrema of the smoothed curve correspond to maxima of the 80–90 yr Gleissberg cycle (Landscheidt, 1983).

The relationships of solar motion and solar activity described by Jose (1965) and Landscheidt (1981, 1983) are not perfect. Jose speculated that the polarity of cycles 20 and 21 might be the same; this was not observed. While he suggested that the period around 1978 might be anomalous, he failed to predict the strong activity maximum that occurred. Landscheidt's (1981) calculated  $\Delta L$  shows no strong impulse at the time of the Wolf minimum (1281–1347) of solar activity.

Perfect agreement of the calculated function and solar activity is only to be expected when all relevant physical interactions are accurately quantified. This is not the case in these studies, where no physical interactions within the Sun are considered. The degree of correspondence found linking the solar variation and the solar inertial motion is in this light remarkable.

## 5. Experimental Rationale and Definitions

Jose (1965) identified a fundamental repetition cycle in the solar inertial motion with a duration of 178.7 yr. This cycle is potentially of considerable interest, as periodicities of this length are found both in the post-1715 observational record of solar activity and in the 10 000-yr  $^{14}\text{C}$  record preserved in tree rings. The endpoints of the Wolf, Spörer, and Maunder minima are also separated by about 180 yr.

The investigation by Jose (1965) covered only a little more than two complete cycles. While he suggested that the solar motion in previous cycles would be very similar, there are reasons to expect some differences. While Jupiter and Saturn exert the largest influence on the solar motion, the effects of Uranus and Neptune are not negligible; and, the configuration of these differs with each successive 179-yr repetition (Jose, 1965, Figure 3).

The present investigation has two primary objectives. First we wish to address the

question of the consistency of the 179-yr cycle of the solar motion over the 13 centuries (A.D. 760–2050) considered previously in the exploratory study by Fairbridge and Sanders (1987). Secondly we employ the perspective gained to look for new relationships linking the solar inertial motion with the occurrence of prolonged minima of solar activity.

To begin with we must review several definitions introduced by Fairbridge and Sanders (1987). As noted earlier they plotted solar orbital cycles beginning and ending with times of the Sun's closest approach to the barycenter ('peribac'). The time of greatest separation of the Sun's center and barycenter for each orbital cycle was determined and labeled 'apobac'. And, in order to characterize the orientation of the orbit in inertial space, they defined an axis of symmetry ('axsym') by drawing a tangent to the two loops of the orbit which intersect near the barycenter (Figure 1), with a perpendicular through the intersection. The angular difference of this perpendicular and  $Y$  describes the orientation of the orbit in space; in Figure 1 the axsym points to  $\alpha = \text{r.a.} = 214^\circ$  (or,  $14^{\text{h}} 16^{\text{m}}$ ).

The axsym bears a conceptual similarity to the line of apsides of planetary orbits (the line connecting the perihelion and aphelion of a planetary orbit, which is the major axis of the orbital ellipse). However, while the apsides of planetary orbits typically rotate slowly in space, the axsym of the solar orbit has a mean retrograde rotation of about  $117.4^\circ$  per orbit. This is linked with the Saturn–Jupiter lap cycle (SJL); each successive conjunction of these bodies takes place roughly  $-117^\circ$  from the previous one, returning to approximately the same part of the range in 3 cycles or about 59.6 yr. If the separation of successive conjunctions were  $120^\circ$  exactly, then the directions of the conjunctions would not change; however, the actual case gives rise to a slow rotation, where 900 yr is the interval between successive conjunctions of Jupiter and Saturn in the same direction in inertial space. In celestial mechanics this is termed the Jupiter–Saturn 'great inequality'.

The period A.D. 760–2050 investigated by Fairbridge and Sanders (1987) includes 66 individual orbital cycles. These show substantial variability in form and duration. Fairbridge and Sanders (1987) subdivided these into 8 classes (A–H), as illustrated in Figure 2. To facilitate comparison the orbits are all plotted with the axsym to the left. Criteria defining the differences of the 8 classes, and the 3 orbit family groupings (cardioid orbits, classes A, B, G, H; right-handed epitrochoid orbits, classes C and E; and left-handed epitrochoid orbits, classes D and F) are given in the legend of Figure 2.

Table IV gives the mean orbital period for each class. This table also lists the frequency of occurrence of each class, the standard deviation of the period, and the mean time of occurrence of the apobac (measured as a decimal fraction of the orbit period), with its associated standard deviation. While the periods of the different orbit classes vary between 15.3 and 23.4 yr, the lengths of the set of orbits of any one class are quite consistent. We will consider the progression of these orbit classes in our intercomparison of earlier and later 179-yr cycles.



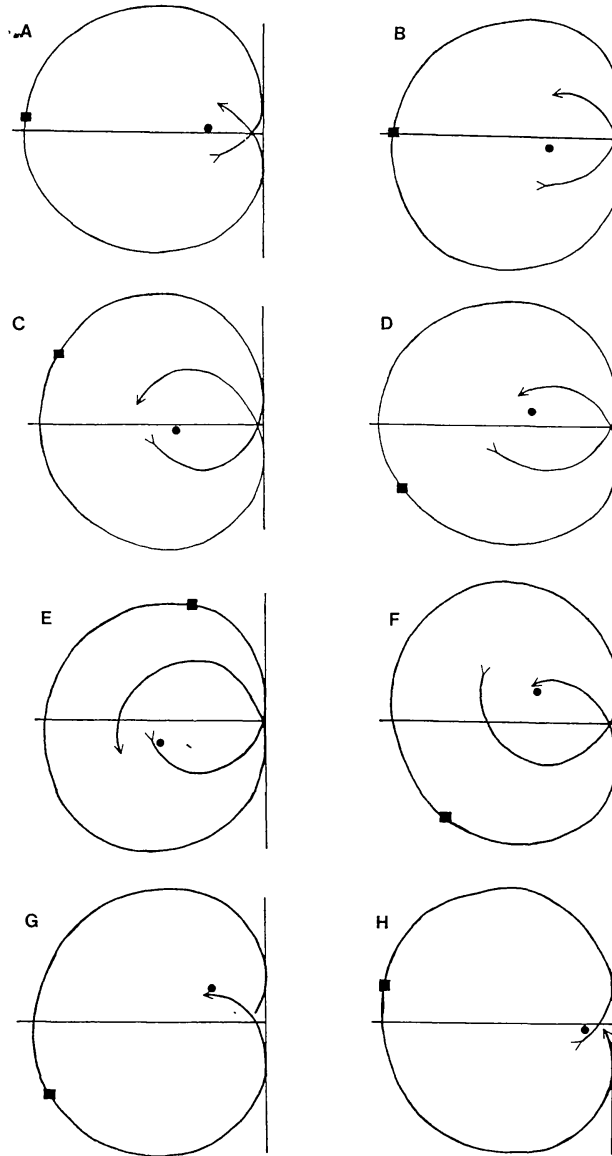


Fig. 2. Orbit classifications. Classes A and B have a high degree of symmetry. Here both the barycenter (●) and the apobac (■) fall close to the axsym (defined in text). The difference between the two is in the position of the peribacs, relative to the barycenter. In class A, the angle peribac<sub>1</sub>-barycenter-peribac<sub>2</sub> is less than 180°, while for class B this angle is close to this value. Classes G and H are similar to classes A and B; however, in these cases there is no crossover of the orbital path. G and H are mirror images of each other. The heart shape of these 4 classes resembles a cardioid. The similarities of classes A–B–G–H permit us to group them as a family. Classes C–F, on the other hand, are epitrochoids (a term defined by Dürer in 1525). All of these are less symmetrical with reference to the axsym. Classes C and D are mirror images; the angle P<sub>1</sub>–B–P<sub>2</sub> in these classes exceeds 180° but does not achieve closure. Classes E and F are similar to classes C and D, except the inner loops very nearly achieve closure. This is the critical difference, for instance, between orbits classed C and E. Note that the near-closure attained in Class E requires a longer time interval for the complete orbit than is the case for class C (Table IV). Classes C and E constitute our second family, designated arbitrarily, right-handed asymmetric orbits. The similar types D and F form the third family of left-handed asymmetric orbits. The examples are: A, 1516–1533; B, 1733–1751; C, 1712–1733; D, 1573–1593; E, 1671–1694; F, 1929–1951; G, 1616–1632; and H, 800–816.

TABLE IV  
Orbit Classes A–H

Class	$n$	Period (yr)	Apobac timing
A	15	$16.33 \pm 0.76$	$0.51 \pm 0.02$
B	8	$18.18 \pm 0.39$	$0.48 \pm 0.03$
C	7	$21.04 \pm 0.93$	$0.42 \pm 0.03$
D	6	$20.37 \pm 0.44$	$0.56 \pm 0.03$
E	17	$23.36 \pm 0.44$	$0.31 \pm 0.02$
F	7	$23.01 \pm 0.72$	$0.68 \pm 0.05$
G	4	$15.35 \pm 0.45$	$0.52 \pm 0.02$
H	2	15.30	$0.48 \pm 0.02$

*Legend:* Orbit period lengths given in years  $\pm \sigma$ . Apobac timing is represented as a decimal fraction of the orbit period,  $\pm \sigma$ . A value of 0.5 in column 4 would mean that the time of greatest orbital radius occurs precisely halfway between the peribacs which define the starting and ending points of each orbit. 200 day step size makes these values approximations only.

## 6. The 179-yr Cycle

To assess the stability of the 179-yr cycle we first produce curves of the variation in the solar barycentric orbit radius  $R$  for the 7 complete 179-yr cycles included in the interval A.D. 816–2054. These curves are presented in Figure 3. It is apparent that the 179-yr cycle in  $R$  is quite similar from one cycle to the next over the time period considered. These curves may be compared with Figures 2(a)–2(b) of Jose (1965). No reliable curve of pre-telescopic sunspot numbers is available for comparison, so we did not derive  $dL/dt$ ,  $dP/dt$ , or  $dT/dt$ .

Next we construct a matrix, where each cell corresponds to one solar orbit and 9 cells arranged horizontally constitute one 179-yr cycle. This matrix is presented in Figure 4.

The information in the individual cells of the matrix of Figure 4 is arranged as follows. At the top is the date of peribac for the beginning of the orbit, in Gregorian calendar years. The number at the bottom of each cell gives the date of the apobac. In the center is the letter designating the orbital class (A–H), as defined above and in Figure 2, along with the orientation (right ascension,  $\alpha$ ) of the axsym in degrees. If desired, one may reconstruct a reasonable approximation of the solar path for any time within the interval of this study, using the patterns provided in Figure 2 and the information given in the matrix of Figure 4.

Examining this matrix we see immediately that the sequence of orbit classes is strikingly similar from one 179-yr cycle to the next. The occasional changes in orbit class noted as we step down any particular column of the matrix almost always involve changes within families; i.e., class D orbits may be followed in subsequent cycles by class F, which is only slightly different. Similarly class H or G may be followed by A or B. There are only four cases where a transition to a different orbital family occurs

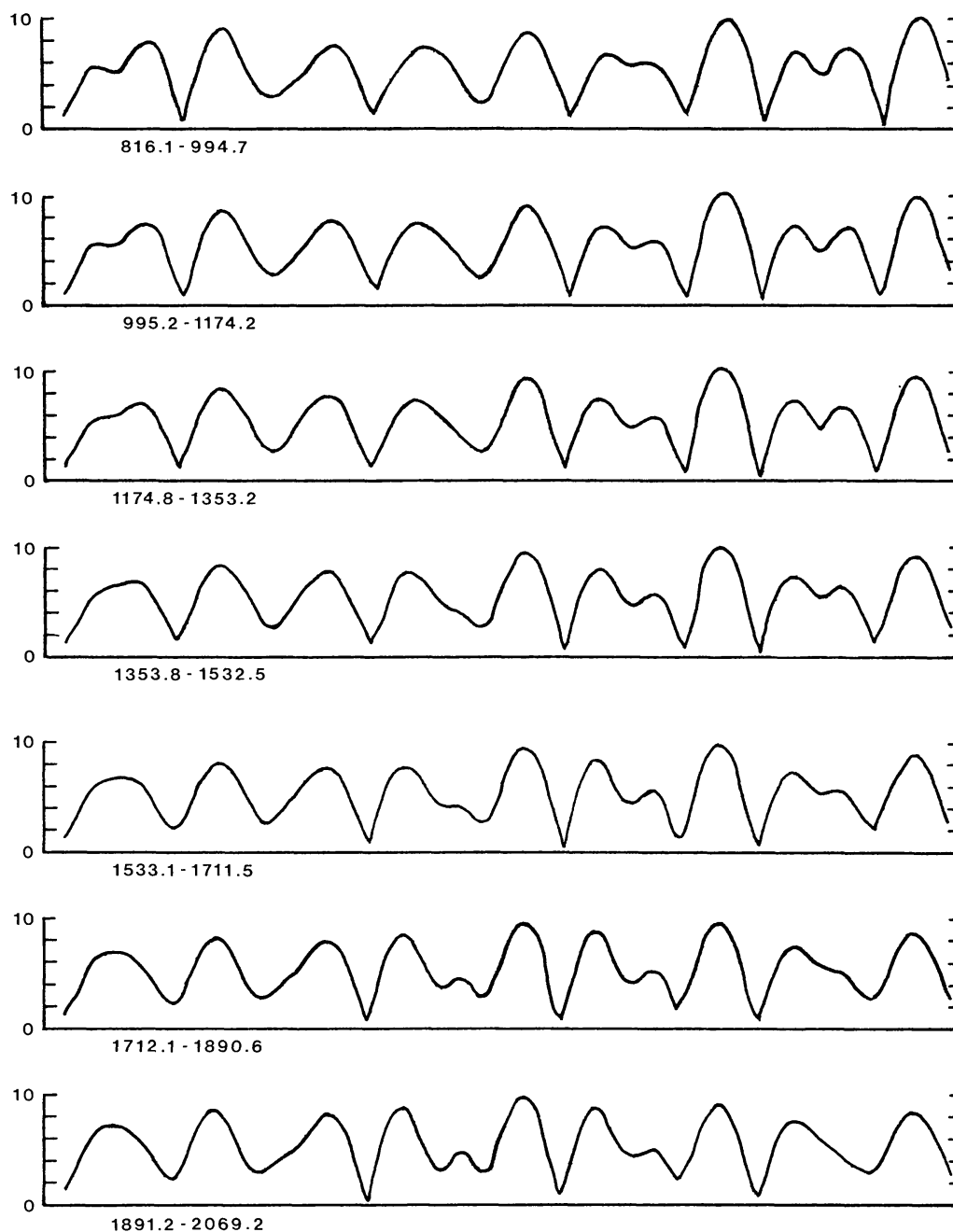


Fig. 3. The 179-yr cycle of the solar barycentric orbit radius  $R$  over 7 cycles beginning in A.D. 816. Units are  $10^{-3}$  AU. The time-period in calendar years for each curve is noted. Successive close approaches to the barycenter (minima of the curve) define the starting and ending points of individual solar orbits of Figures 1 and 2.

(956.3–1134.8, F–E; 1018.7–1197.2, B–C; 1197.2–1376.3, C–B; 1353–1533, F–C). Table V lists statistical results for the column groupings of the matrix of Figure 4. All but 2 of the orbit period standard deviations are  $< 1$  yr.

In general Jose's (1965) expectation that the pattern of the solar motion would be similar in earlier 179-yr cycles has been confirmed. We note (as he did) that over long

						761.4 A 303 769.6	777.2 F 211 794.0	800.8 H 71 808.0
816.1 F 330 833.0	839.7 B 198 847.8	857.7 D 85 870.3	878.5 C 330 887.0	899.3 B 210 908.0	917.4 E 98 925.0	940.4 A 332 948.6	956.3 F 223 973.3	979.9 H 100 987.5
995.2 F 350 1011.6	1018.7 B 229 1026.9	1037.3 D 108 1048.3	1057.6 C 349 1065.7	1078.4 B 240 1087.7	1096.5 E 116 1103.0	1119.5 A 2 1127.7	1134.8 E 243 1141.4	1158.4 A 125 1166.6
1174.8 F 10 1189.0	1197.2 C 258 1205.9	1216.4 D 132 1227.4	1236.1 C 20 1244.3	1258.0 A 268 1267.3	1275.0 E 132 1282.1	1298.5 A 36 1305.7	1313.9 E 260 1321.5	1337.4 A 154 1345.6
1353.8 F 30 1367.5	1376.3 B 282 1385.0	1394.9 D 159 1405.8	1415.2 E 37 1422.7	1437.6 A 293 1446.4	1454.0 E 146 1460.0	1477.6 A 73 1485.4	1493.1 E 280 1499.7	1516.1 A 185 1524.3
1533.1 C 54 1543.3	1555.0 B 303 1563.7	1573.6 D 186 1585.1	1593.8 E 54 1601.0	1616.8 G 320 1625.0	1632.7 E 161 1639.8	1656.3 A 89 1664.5	1671.6 E 295 1678.7	1694.6 A 210 1703.0
1712.1 C 82 1721.0	1733.5 B 322 1742.3	1751.5 D 216 1764.0	1772.4 E 72 1780.1	1796.4 G 350 1804.1	1811.2 E 185 1818.4	1835.3 G 110 1842.9	1850.7 E 317 1858.3	1873.7 A 237 1882.4
1891.2 C 100 1900.5	1912.5 A 343 1920.7	1929.5 F 247 1943.7	1951.4 E 91 1958.5	1975.0 G 20 1983.2	1990.3 E 214 1997.4	2013.8 A 139 2021.8	2030.3 E 346 2037.9	2052.2 B 261 2061.5

Fig. 4. Orbit matrix. Each row of this matrix corresponds to one 179-yr repetition of the fundamental cycle described by Jose (1965). Each cycle consists of 9 solar orbits. Each row corresponds to one of the curves of Figure 3. The orbit class (A–H) and axsym orientation (r.a.,  $\alpha$ ) are noted in the center of each cell; the date of the first peribac is found at the top, and the bottom number gives the date of the apobac for the orbit. Orbits of prolonged sunspot minima are outlined.

TABLE V  
Orbit matrix statistics (columns)

Column	Period (yr)	Apobac timing
1	$22.37 \pm 0.92$	$0.57 \pm 0.13$
2	$18.29 \pm 0.70$	$0.46 \pm 0.02$
3	$20.59 \pm 0.70$	$0.58 \pm 0.04$
4	$22.36 \pm 1.27$	$0.35 \pm 0.04$
5	$16.51 \pm 1.30$	$0.52 \pm 0.02$
6	$23.47 \pm 0.38$	$0.30 \pm 0.02$
7	$15.63 \pm 0.41$	$0.51 \pm 0.02$
8	$23.37 \pm 0.32$	$0.41 \pm 0.19$
9	$16.61 \pm 0.93$	$0.49 \pm 0.02$

Legend: Orbit periods in years  $\pm \sigma$ . Apobac timing given as a decimal fraction of the orbit period  $\pm \sigma$ . 200 day step size makes these values approximations only.

time periods some differences are to be expected; compare for instance the earliest and most recent curves of Figure 3.

## 7. Solar Motion and Prolonged Minima

Prolonged minima are outlined in Figure 4. Table II gives the designations and adopted dates for these episodes.

We have uncovered two patterns in the series of axsym values (listed in the center of each cell of the matrix) which bear a relationship to the prolonged minima. Neither of these in isolation constitutes a reliable predictor, but together they appear to explain (1) the placement of the minima within the 13-century interval, (2) the approximate 180-yr spacing of the minima, and (3) the timing of the onset, duration, and termination of each prolonged minimum.

The first of these parameters is the difference of successive values ( $\Delta_{\text{axsym}}$ ). These differences are listed in Table VI. As noted earlier the axsym has an average retrograde rotation of  $117.4^\circ$  per orbit. The amount of this rotation, however, ranges from  $71^\circ$  to  $165^\circ$  during the time interval of this investigation. Figure 5 is a graphic projection of the series of differences of Table VI. The shaded portions of this figure represent the prolonged minima of solar activity of Table II. The abbreviated shaded area represents the Sabine excursion, from 1798–1823; for reasons to be elaborated we have also shaded the period beyond 1990.

TABLE VI

$\Delta_{\text{axsym}}$   
(Amplitude of inertial rotation of orbital axis of symmetry)

761.4	92	1197.2	126	1632.7	72
777.2	140	1216.4	112	1656.3	154
800.8	101	1236.1	112	1671.6	85
816.1	132	1258.0	136	1694.6	128
839.7	113	1275.0	96	1712.1	120
857.7	115	1298.5	136	1733.5	106
878.5	120	1313.9	104	1751.5	144
899.3	112	1337.4	124	1772.4	82
917.4	126	1353.8	108	1796.4	165
940.4	109	1376.3	123	1811.2	75
956.3	123	1394.9	122	1835.3	153
979.9	110	1415.2	104	1850.7	80
995.2	121	1437.6	147	1873.7	137
1018.7	121	1454.0	73	1891.2	117
1037.3	119	1477.6	153	1912.5	96
1057.6	109	1493.1	95	1929.5	156
1078.4	124	1516.1	131	1951.4	71
1096.5	114	1533.1	111	1975.0	166
1119.5	119	1555.0	117	1990.3	75
1134.8	118	1573.6	132	2013.8	153
1158.4	115	1593.8	94	2030.3	85
1174.8	112	1616.8	159	2052.2	

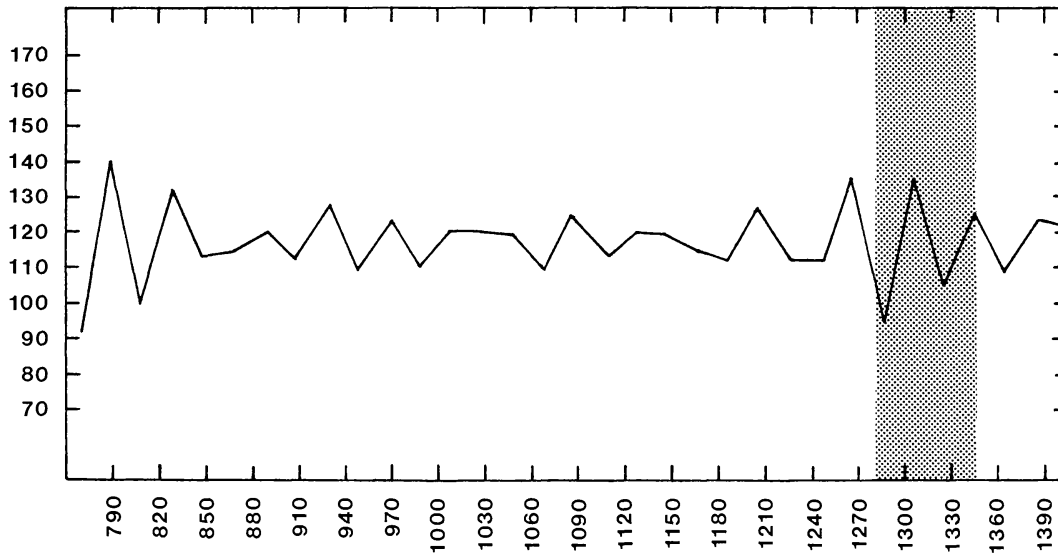


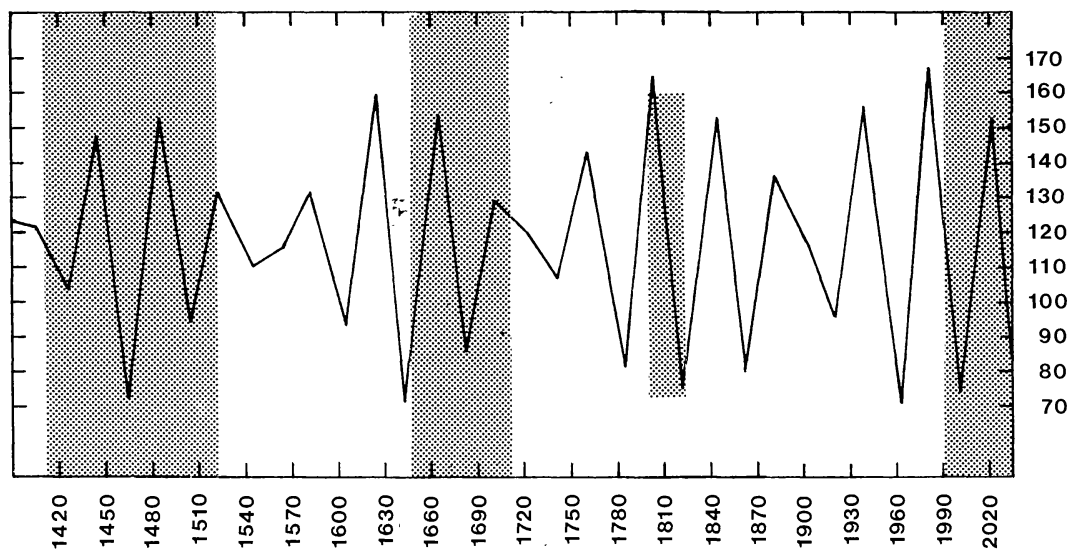
Fig. 5.  $\Delta_{\text{axsym}}$ . This curve represents the differences of orbit axsym orientations (Table VI) from one solar orbit to the next; the first value,  $92^\circ$ , is for instance the difference of axsym values for the orbits beginning in 761.4 and 777.2 ( $303^\circ - 211^\circ$ ). Calendar years are indicated on the ordinate. Prolonged minima of sunspot

Each of the prolonged minima is associated in time with an episode of large fluctuations of  $\Delta_{\text{axsym}}$ . However, there are differences in the time of inception of the minimum, relative to the curve; we will discuss these in connection with our second criterion. Physically, a large rotation of the orbit axis in inertial space implies relatively large values of the curvature parameters  $\rho$  and  $dP/dt$  in the minor loops of the orbit near the barycenter (Figure 1), along with larger values of the torque parameters  $dL/dt$  and  $dT/dt$  (Landscheidt, 1981, 1983). Thus the correspondence of large  $\Delta_{\text{axsym}}$  fluctuations and the Spörer and Maunder minima is consistent with the relationship to  $\Delta L$  reported by Landscheidt (1981).

The times of large fluctuation of the  $\Delta_{\text{axsym}}$  curve are separated in time by about 180 yr. The larger fluctuations are absent in the interval A.D. 850–1250, but the episode near A.D. 760 is in phase with those after 1250. This feature of the 179-yr repetition cycle of the solar inertial motion was previously unknown.

The direction of the orbit axsym in inertial space is the second parameter showing an apparent relationship to the occurrence of the prolonged minima. Figure 6(a) gives the distribution of orbit axsym values for the 15 solar orbits during the Wolf, Spörer, and Maunder minima. This distribution shows a preference for angular values between about  $120^\circ$  and about  $300^\circ$ ; 11 of the 15 axsym directions are found in this range. For comparison the orbit axsym values for periods of high solar activity (Table I) are plotted in Figure 6(b); 8 of the 10 high activity axsym values are found in the opposite hemisphere of the range.

A moment's reflection yields the insight that any series of angular values spaced by about  $120^\circ$  must necessarily include runs where values in one or the other of these  $180^\circ$  ranges must predominate, with a ratio of about 2 to 1. Inspection of the matrix of Figure 4 reveals that high activity range axsym values predominate in the years



activity are shaded. The abbreviated shaded period is the Sabine excursion of 1798–1823; reasons for shading the period beyond 1990 are summarized in section 8.

761–1134, 1533–1632, and 1712–1990. Low activity range axsym values predominate throughout all of the prolonged minima and in the period 1134–1258 (immediately preceding the Wolf minimum). Low activity range axsym values of Figure 4 are underlined to highlight this pattern. It takes about 900 yr to complete a cycle, where first low and then high activity axsym ranges predominate. This cycle originates in the 900-yr ‘great inequality’ of the motion of Jupiter and Saturn. We note in passing that Henkel (1972) has suggested an ‘ultra-long cycle of solar activity’ with duration  $\approx 900$  yr. The

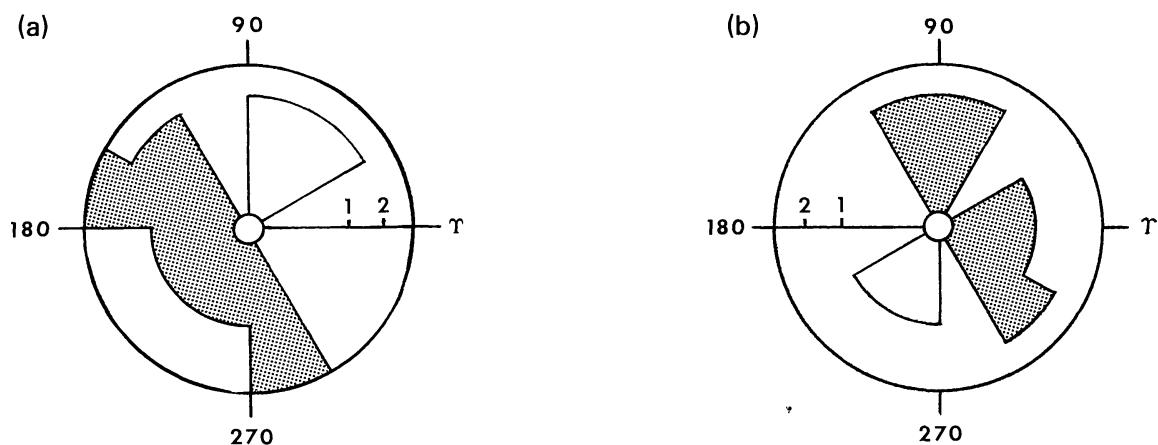


Fig. 6. Axsym distributions for prolonged minima and for periods of high sunspot activity ( $R_M > 100$ ) since A.D. 1700. (a) is a clock diagram showing the distribution of axsym directions for the 15 orbits of Figure 4 associated with prolonged minima of sunspot activity. In this equal area projection the radius of each  $30^\circ$  sector is proportional to  $\sqrt{n}$ , where  $n$  is the count of values found there. A scale of values is provided. Eleven of the 15 axsym directions for the orbits during solar prolonged minima (Figure 4) cluster in the range  $120^\circ$ – $300^\circ$ . (b) is a similar diagram giving the distribution of axsym directions for the 10 orbits characterized by high levels of solar activity since 1700 (Table I). In this case 8 of 10 orbit axsym directions cluster opposite the preferred range of the prolonged minima of (a).

large fluctuations of  $\Delta_{\text{axsym}}$  give rise to some irregularity in this long-period cycle of axsym orientations.

We note that any shifting of the block of prolonged minima orbits of Figure 4, forward or backward in time, degrades the pattern present in Figure 6(a). The correspondence in time of prolonged minima and periods with axsym values falling predominantly in the range  $120\text{--}300^\circ$  is factual. The clustering of 8 of 10 high activity orbits in the opposite part of the range (Figure 6(b)) suggests that we may be seeing something of physical significance.

Having identified two less-than-perfect possible relationships of the solar inertial motion and prolonged minima, it remains to see how well these together explain the distribution of prolonged minima in time.

For the period previous to A.D. 1134 high activity range axsym values predominate (13/19) and  $\Delta_{\text{axsym}}$  fluctuations are small. The brief and relatively weak Oort episode falls within this interval, but no prolonged minimum occurred.

From 1134–1275 low activity range axsym values predominate, but large fluctuations of  $\Delta_{\text{axsym}}$  are absent. No prolonged minimum occurred.

Large fluctuations of  $\Delta_{\text{axsym}}$  and axsym orientations in the low activity range coincide for the first time in the period beginning with the orbit of A.D. 1275. The Wolf minimum (1281–1347) occurs. The minimum is terminated with the return to smaller fluctuations of the  $\Delta_{\text{axsym}}$  curve, which characterizes the brief period between the Wolf and Spörer minima.

Larger amplitude fluctuations of  $\Delta_{\text{axsym}}$  are initiated at the beginning of the Spörer minimum. The unusual duration of this episode (120 yr) has been commented on previously (Stuiver and Quay, 1981; Stuiver, 1981). We note that at this point low activity range axsym values have predominated for nearly 3 centuries previously. This condition continues until the end of the Spörer minimum.

From 1533–1632 high activity range axsym values predominate and  $\Delta_{\text{axsym}}$  fluctuations are initially small, though subsequently increasing. This period is thought to have been characterized by normal solar activity.

During the interval 1632–1712 large fluctuations of  $\Delta_{\text{axsym}}$  are present and there is a brief return to axsym values predominantly in the low activity range (3/4). The Maunder minimum occurs.

We note that all three of the prolonged minima end under similar conditions, i.e., with reduced amplitude  $\Delta_{\text{axsym}}$  fluctuations, during orbits with axsyms oriented in the high activity range.

From 1712–1990 axsym values in the high activity range predominate (10/14). Large fluctuations of  $\Delta_{\text{axsym}}$  occur but no prolonged minimum is initiated as the orientation criterion is not met. The Sabine excursion occurs during the period of largest amplitude fluctuations of  $\Delta_{\text{axsym}}$ .

Thus the principal prolonged minima of solar activity of the current millenium have occurred when both of our derived criteria are met, and at no other times. Periods of normal solar activity during the time period of our study occur only when these two conditions are not fulfilled.



## 8. Prediction and ‘Retrodiction’

The conditions for the occurrence of a prolonged minimum of solar activity obtained in the previous section may be easily applied in retrodicting past activity and in predicting future activity. Note for instance in Figure 5 the suggestion of a previous period of large fluctuations of  $\Delta_{\text{axsym}}$ , in the eighth century A.D. Preliminary work shows that axsym orientations for several orbits before A.D. 760 fall in the low activity range. Thus we should expect to encounter another prolonged minimum in this period, as both criteria appear to be satisfied. The radiocarbon record confirms the existence of a prolonged minimum in this time period (Clarke, 1979; Stuiver and Quay, 1981). We will study the solar motion for previous millenia at a later date. (Considerable time and effort is required to obtain accurate solutions for outer planet motions in remote times.)

Our criteria are certainly not the last word on the subject. While the agreement for the period studied is good, the axsym parameter is a relatively crude parameterization of dynamical aspects of the motion. And, the sample of events is small and the statistical significance of the patterns found is difficult to evaluate. We note that our parameters do not predict any significant fluctuation near A.D. 1020, whereas auroral and radiocarbon records suggest a brief period of suppressed solar activity at this time. Thus some caution is indicated.

While we are aware of the risks involved in making predictions on the basis of limited data, we must note that both criteria for the occurrence of a prolonged minimum of solar activity are met beginning in 1990. Figure 5 shows that we are within a period of large fluctuations of  $\Delta_{\text{axsym}}$ . Beginning with the orbit of 1990 we enter the phase wherein low activity range axsym values predominate. Based on the known behavior of the Sun over the past 13 centuries, we suggest that a new prolonged minimum of solar activity may be imminent. This prediction agrees with that of Landscheidt (1981), who has shown that the values of  $\Delta L$  reached around 1990 will be greater than at any other time since the 1660’s.

Our tentative prediction is for the inception of a new prolonged minimum within the time span of the solar barycentric orbit of 1990–2013. While our results provide no basis for predictions on time scales of 1–5 years, nevertheless it is of interest to make note of several short-term predictions made by other authors. On the one hand there are the predictions of Landscheidt (1981, 1983), Fairbridge and Hameed (1983), Otaola and Zenteno (1983), Gregg (1984), and Rabin *et al.* (1986), wherein the 179-yr cycle or other long-term patterns are taken into account. These authors all suggest that cycle 21 should be longer than usual, reaching its minimum late in the present decade or in 1990. Most of these authors further suggest that cycle 22, predicted to peak near 1995, will be characterized by unusually low solar activity at maximum. On the other hand there are the predictions of Schatten and Hedin (1984) and Bracewell (1986), wherein cycle 22 is expected to peak near 1990, with smoothed sunspot numbers  $> 100$ . These disagreements lend added interest for those monitoring the evolution of solar activity over the next few years.

We have extended our investigation beyond the time interval of the earlier study by

Fairbridge and Sanders (1987), to A.D. 2100. The peribac dates of the next two orbits are September 2069 and January 2091; the axsyms point to  $126^\circ$  and  $7^\circ$  respectively.  $\Delta_{\text{axsym}}$  values are  $135^\circ$  for 2052–2069 and  $119^\circ$  for 2069–2091. Thus the combination of small  $\Delta_{\text{axsym}}$  fluctuations and a high activity range axsym value of  $7^\circ$  should terminate the predicted prolonged minimum in about 2091.

## 9. Discussion

The basic implication of a relationship of solar motion and solar activity is that some mechanism related to the motion in some way alters or modulates material flows and/or magnetic fields within the rotating Sun, thereby accounting for the relationships found. There is now a considerable body of evidence to support this (Section 4). The several planetary positional and planetary synodic period resonance correlations cited earlier are more consistent with a dynamical mechanism than with a tidal mechanism, as in a majority of cases periodicities and resonances of tidally ineffective planets are noted.

Newtonian gravitation theory, however, stipulates that the tides are the only gravitational phenomenon acting to stress or distort the body of the Sun; the solar motion is ignored. We do not propose to address this question of discrepancies between theory and observation at this time.

## 10. Conclusions

The inertial orientation of the solar orbit and the amplitude of the precessional rotation of the orbit each bear a relationship to the occurrence of the principal prolonged minima of solar activity of the current millenium. While the present investigation has a number of limitations, still we are aware of no other approach to the problem of the temporal distribution of prolonged minima yielding comparable agreement, save that of Landscheidt (1981, 1983), who employed a somewhat different methodology in studying the same relationship.

We have derived a set of conditions for the occurrence of prolonged minima which provide a basis for the retrodiction of past episodes and the prediction of future ones. Our prediction of an imminent prolonged minimum of solar activity may have significant implications for observational solar astronomy and for society at large, due to the possible relationship of long-term fluctuations of solar activity and climate.

*Note:* The set of programs for resolving the solar motion relative to the ecliptic, equatorial, and invariable planes described in Section 3 will be made available to interested parties on request. The programs are written in IBM BasicA. Please contact the second author for information.

## Acknowledgements

We thank T. M. L. Wigley, T. Landscheidt, P. M. Kelly, and S. Hameed for critical comments on an earlier version of this study, and J. Blizard, M. Stuiver, and E. M. Standish Jr. for supplying needed information.

## References

- Arriaga, N.: 1955, *J. Geophys. Res.* **60**, 535.
- Bagby, J. P.: 1975, *Nature* **253**, 482.
- Barton, C. E., Merrill, R. T., and Barbetti, M.: 1979, *Phys. Earth Planetary Int.* **20**, 96.
- Bigg, E. K.: 1967, *Astron. J.* **72**, 463.
- Blizard, J. B.: 1981, *Bull. Am. Astron. Soc.* **13**, 876.
- Bracewell, R. N.: 1986, *Nature* **323**, 516.
- Bureau, R. A. and Craine, L. B.: 1970, *Nature* **228**, 984.
- Clark, D.: 1979, *New Sci.* **168**.
- Clark, D. and Stephenson, F. R.: 1978, *Quart. J. Roy. Astron. Soc.* **19**, 387.
- Clemence, G. M.: 1953, *Astron. Pap. Am. Ephemeris* **13**, Pt. 4.
- Cohen, T. J. and Lintz, P. R.: 1974, *Nature* **250**, 398.
- Cole, T. W.: 1973, *Solar Phys.* **30**, 103.
- Currie, R. G.: 1973, *Astrophys. Space Sci.* **20**, 509.
- Damon, P. E.: 1977, in J. Zirker (ed.), *Coronal Holes and High-Speed Streams*, Colo. Assoc. Univ. Press, p. 429.
- Damon, P. E. and Linick, T.: 1986, *Radiocarbon* **28**, No. 2A, 266.
- de Jong, A. F. M., Mook, W. G., and Becker, B.: 1979, *Nature* **280**, 48.
- de Jong, A. F. M. and Mook, W. G.: 1980, *Radiocarbon* **22**, 267.
- de la Rue, W., Stewart, B., and Loewy, B.: 1872, *Proc. Roy. Soc. London* **20**, 210.
- de Vries, H. L.: 1958, *Koninklijke Nederlandse Akad. Wetensch. Proc. Ser.* **B61**, 94.
- Dingle, L. A., Van Hoven, G., and Sturrock, P. A.: 1973, *Solar Phys.* **31**, 243.
- Eddy, J. A.: 1976, *Science* **192**, 1189.
- Eddy, J. A.: 1977, in O. R. White (ed.), *The Solar Output and Its Variation*, Colo. Assoc. Univ. Press, p. 51.
- Eddy, J. A.: 1983, *Solar Phys.* **89**, 195.
- Fairbridge, R. W. and Hameed, S.: 1983, *Astron. J.* **88**, 867.
- Fairbridge, R. W. and Sanders, J. E.: 1987, in J. E. Sanders and M. Rampino (eds.), *History, Periodicity, Predictability*, Van Nostrand Reinhold (in press).
- Ferris, G. A. J.: 1969, *J. Brit. Astron. Assoc.* **79**, 385.
- Gregg, D. P.: 1984, *Solar Phys.* **90**, 185.
- Henkel, R.: 1972, *Solar Phys.* **25**, 498.
- Jose, P. D.: 1965, *Astron. J.* **70**, 193.
- Klein, J., Lerman, J. C., Damon, P. E., and Linick, T.: 1980, *Radiocarbon* **22**, 950.
- Klein, J., Lerman, J. C., Damon, P. E., and Ralph, E. K.: 1982, *Radiocarbon* **24**, 103.
- Kuklin, G. V.: 1976, 'Basic Mechanisms of Solar Activity', in V. Bumba and J. Kleczek (eds.), *IAU Symp.* **71**, 147.
- Landscheidt, T.: 1981, *J. Interdiscipl. Cycl. Res.* **12**, 3.
- Landscheidt, T.: 1983, in B. M. McCormac (ed.), *Weather and Climate Response to Solar Variations*, Colo. Assoc. Univ. Press.
- Lazear, G., Damon, P. E., and Sternberg, R.: 1980, *Radiocarbon* **22**, 318.
- Lomb, N. R. and Andersen, A. P.: 1980, *Monthly Notices Roy. Astron. Soc.* **190**, 723.
- Maunder, E. W.: 1894, *Knowledge* **17**, 173.
- Mörth, H. T., and Schlamminger, L.: 1979, in B. M. McCormac and T. Seliga (eds.), *Solar-Terrestrial Influences on Weather and Climate*, D. Reidel Publ. Co., Dordrecht, Holland, p. 193.
- Neftel, A., Oeschger, H., and Suess, H. E.: 1981, *Earth Planetary Sci. Letters* **56**, 127.
- Nelson, J. H.: 1951, *RCA Review* **12**, 26.
- Nelson, J. H.: 1954, *Trans. Inst. Rad. Eng.* **CS-2**, 19.
- Newhall, X. X., Standish, E. M., Jr., and Williams, J. G.: 1983, *Astron. Astrophys.* **125**, 150.
- Okal, E. and Anderson, D. L.: 1975, *Nature* **253**, 511.
- Otaola, J. A. and Zenteno, G.: 1983, *Solar Phys.* **89**, 209.
- Pearson, G. W., Pilcher, J. R., and Baillie, M. G. L.: 1983, *Radiocarbon* **25**, 179.
- Pimm, R. S. and Bjorn, T.: 1969, *Prediction of Smoothed Sunspot Numbers Using Dynamic Relations Between the Sun and Planets*, NASA N69-29781, Washington, D.C.
- Rabin, D., Wilson, R. H., and Moore, R. L.: 1986, *Geophys. Res. Letters* **13**, 352.
- Schatten, K. H., and Hedin, A. E.: 1984, *Geophys. Res. Letters* **11**, 873.

- Schove, D. J.: 1983, *Sunspot Cycles*, Hutchinson-Ross.
- Schuster, A.: 1911, *Proc. Roy. Soc. London* **85**, 309.
- Siegenthaler, U., Heimann, M., and Oeschger, H.: 1980, *Radiocarbon* **22**, 177.
- Siscoe, G. L.: 1980, *Rev. Geophys. Space Phys.* **18**, 647.
- Smythe, C. M. and Eddy, J. A.: 1977, *Nature* **266**, 434.
- Sonett, C. P.: 1982, *Geophys. Res. Letters* **9**, 1313.
- Sonett, C. P.: 1984, *Rev. Geophys. Space Phys.* **22**, 239.
- Sonett, C. P. and Suess, H. E.: 1984, *Nature* **307**, 141.
- Stuiver, M.: 1961, *J. Geophys. Res.* **66**, 273.
- Stuiver, M.: 1980, *Nature* **286**, 868.
- Stuiver, M.: 1982, *Radiocarbon* **24**, 1.
- Stuiver, M.: 1983, *Radiocarbon* **25**, 219.
- Stuiver, M.: 1986, personal communication.
- Stuiver, M. and Grootes, P. M.: 1980, in R. O. Pepin, J. A. Eddy and K. T. Merrill (eds.), *Proc. Conf. Ancient Sun*, p. 165.
- Stuiver, M. and Pearson, G. W.: 1986, *Radiocarbon* **28**, 805.
- Stuiver, M. and Quay, P. D.: 1980a, *Science* **207**, 11.
- Stuiver, M. and Quay, P. D.: 1980b, *Radiocarbon* **22**, 166.
- Stuiver, M. and Quay, P. D.: 1980c, *Solar Phys.* **74**, 479.
- Suda, T.: 1962, *J. Meteorol. Soc. Japan* **40**, 287.
- Suess, H. E.: 1980, *Radiocarbon* **22**, 200.
- Suess, H. E.: 1986, *Radiocarbon* **28**, 259.
- Takahashi, K.: 1968, *Solar Phys.* **3**, 598.
- Van Flandern, T. C. and Pulkkinen, K. F.: 1979, *Astrophys. J. Suppl.* **41**, 391.
- Wittmann, A.: 1978, *Astron. Astrophys.* **66**, 93.
- Wood, K. D.: 1972, *Nature* **240**, 91.
- Wood, R. M.: 1975, *Nature* **255**, 312.
- Wood, R. M. and Wood, K. D.: 1965, *Nature* **208**, 129.